Noncontacting lateral transportation using gas squeeze film generated by flexural traveling waves—Numerical analysis

Adi Minikes[a)]
Faculty of Mechanical Engineering, Haifa 32000, Technion, Israel

Izhak Bucher[b)]
Dynamics & Mechatronics Laboratory, Faculty of Mechanical Engineering, Haifa 32000, Technion, Israel

(Received 29 July 2002; revised 24 January 2003; accepted 10 February 2003)

This paper presents the theory describing the dynamical behavior of a noncontacting lateral transportation of planer objects by means of a gas squeeze film created by traveling flexural waves of a driving surface. An oscillating motion in the normal direction between two surfaces can generate a gas film with an average pressure higher than the surrounding. This load-carrying phenomenon arises from the fact that a viscous flow cannot be instantaneously squeezed; therefore, fast vibrations give rise to a cushioning effect. Equilibrium is established through a balance between viscous flow forces and compressibility forces. When the oscillatory motion between two surfaces creates traveling waves, lateral viscous forces are generated in addition to the normal levitation forces. These forces are produced as a result of nonuniform pressure gradients in the lateral direction between the surfaces. The combination of normal and lateral forces could be used for transporting objects without any direct contact with the driving surface. The numerical algorithm in this work couples the squeeze film phenomenon, which is represented by means of finite difference equations, to model a variant of the Reynolds equation, together with the equations describing the dynamics of the floating object. Numerical simulations are presented and investigated to highlight noteworthy topics. [DOI: 10.1121/1.1564014]

PACS numbers: 43.25.Uv, 43.25.Op [MFH]

I. INTRODUCTION

In previous papers dealing with squeeze film and air bearings that are created by normal vibration between two vibrating surfaces, the analysis was carried out for the case where the mean clearance between the surfaces was predetermined.[1,2] In other words, the vibrating surface was brought (numerically) close to a fixed surface to achieve a prescribed clearance. When trying to model an applicative problem such as squeeze bearing or mass levitation, where the clearance cannot be fixed but is determined by equilibrium of forces, the analysis appearing in the literature is not suitable.

Several studies have been carried out in the field of acoustics describing the near-field levitation phenomenon.[3–5] While in a linear medium the acoustical impedance is constant since the pressure and the velocity are linearly related, in a nonlinear medium the acoustic impedance varies in time, producing a mean acoustic pressure. When an unconfined surface oscillates in a sufficiently high frequency such that the wavelength is small in comparison to the typical length of the surface, an unbounded acoustic wave is produced. If a plane target is placed in the path of such unbounded acoustic beam, the time-average pressure (defined as the Langevin radiation pressure) exerted on the target creates a levitation force. In conventional acoustic levitation, standing waves are formed between a radiating source and a reflector, and the levitation takes place near the pressure nodes in the field. In the case dealt with here, the levitated planar object acts as a reflector. In this situation the closer the object approaches the radiating source the larger the levitation force becomes.

In systems such as the one presented here, the clearance between the surfaces may be uneven; hence, the film thickness may be spatially nonuniform. As the pressure gradients and the velocity gradients in the film depend on the shape of the acoustic field, the gradients will be nonuniform as well. Therefore, in addition to normal acoustic radiation force performing the levitation, there are also acoustic viscous forces in the tangential directions. The streaming of the medium created by the radiation pressure gradients is balanced by viscous losses associated with the boundaries of the medium which create relative motion between adjacent portions of the medium producing shear deformation.

Recently, Hashimoto *et al.* have studied experimentally a method of transporting an object by exciting traveling flexural vibration waves along a plate.[3] Their experiment has confirmed the phenomenon that objects could be transported without contact. Unfortunately, in their work, a model or a numerical theory to describe the physical mechanism of the system is not provided. In addition, the parameters of the experiment were not fully investigated, leaving several inconsistencies in the results.

The present work suggests a different approach for solving the pressure field between the vibrating surface and the levitated object, which is not based on the commonly used acoustic approximation equations. Instead of solving a second-order approximations for Navier–Stokes equation in order to describe the acoustic streaming, we derive a modified nonlinear compressible Reynolds equation (which, in a

a)Electronic mail: minikes@technion.ac.il
b)Electronic mail: bucher@technion.ac.il

 0001-4966/2003/113(5)/2464/10/$19.00

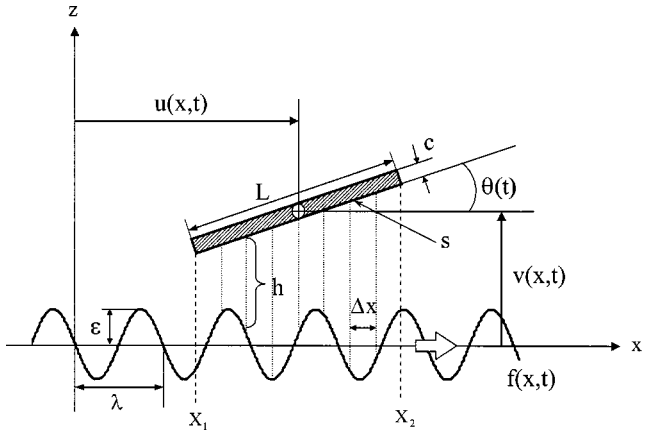

FIG. 1. Schematic layout of the system.

similar manner to acoustic equations, is derived from Navier–Stokes equations) based on a fluid mechanics approach.

This work begins by presenting the physical system and describing the governing equations of the system. Later, the numerical procedure employed for solving the coupled equations is described with suitable variable scaling and transformations. Then, we present a numerical parametric study examining the effect of the terminal speed and the nature of the traveling excitation wave on the dynamics. In the last section we discuss the influence of the acoustic radiation pressure, generated by the vibrating surface, on the boundary conditions of the squeeze film.

II. DERIVATION OF THE EQUATIONS OF MOTION

In this section the equations of motion of the overall system are developed. First, we deal with the dynamics of the squeeze film and discuss the prevailing variables. Later, the modified nonlinear compressible Reynolds equation is derived and the importance of each term is evaluated. The kinematical boundary conditions are outlined and with the dynamics of the floating object, the coupled equations of motions are developed.

Consider the case illustrated in Fig. 1, where a planar object is modeled as a rigid plate having length (L), width (b), thickness (c), and weight (m). The object is levitated and transported by a squeeze film created between the plate (s) and a traveling vibration wave that is shown on the lower surface (f). The traveling wave propagates in the positive x direction, oscillating at a frequency (ω) with an amplitude (ε) and a wavelength (λ), while the plate being rigid can be modeled using three coordinates (u,v,θ).

The fluid dynamics in the squeeze film is numerically modeled by means of finite difference equations. Since the plate is moving, the geometrical boundaries of the squeeze film are defined by the coordinates (x_1,x_2,y_1,y_2). These are determined by the geometry of the plate (L,b), the position of the plate's center of gravity (u,v), and the plate's angle of inclination (θ). The local film thickness (h) is defined by the local gap between the surfaces using spatial finite steps (Δx). For simplicity, in this paper the traveling wave progresses only in one dimension (the x direction); consequently, the pressure gradients in the y direction are symmetrical. Due to symmetry the total lateral force in the y direction vanishes, but in cases where the plate's width and length (b,L) are of the same order of magnitude, the edge effects on the gas flow in the y direction are not negligible and should be considered. In such cases the gas squeeze film needs to be treated as a two-dimensional flow (x,y plane), even though there is no motion of the plate in the y direction.

A. Reynolds equation for squeeze film

In this section we briefly derive the differential equation governing the squeeze film phenomena with some modifications for the presented case. From the modified Reynolds equation we can obtain the pressure distribution and the velocity profile in the film for determining the reactions forces excreted on the levitated plate.

In order to allow the load-carrying phenomenon to take place, the bearing dimension (L), which represents a typical length of the involved surfaces, must be much greater than the thickness of the squeezed film (h). If this restriction does not apply, the effects in the boundaries will prevent the increase of the mean pressure in the film compared to the surrounding. Furthermore, the velocity of the fluid in the normal direction is of an order of h/t and the velocities of the fluid in the lateral directions are of an order L/t, where t is the time period of the normal oscillations. Therefore, as $L \gg h$, the normal velocity of the fluid is relatively neglected compared with the lateral velocities.

Performing an order of magnitude analysis on the differential equations representing the momentum of the fluid (Navier–Stokes) and neglecting the normal velocity in the fluid reveals that the pressure gradient in the normal direction is of the order h (film thickness), while the pressure gradients in the lateral directions are of the order of unity (normalized).[6] Such typical magnitudes may suggest that the pressure gradient in the normal direction could be ignored.

For the sake of discussion, the analysis of the fluid mechanics part of the squeeze film phenomenon takes into account only the momentum in the one lateral dimension. A more complete analysis is introduced later on.

Under the above assumptions, the momentum equation in an x direction for a two-dimensional Newtonian flow reduces to

$$\rho\left(\frac{\partial v_x}{\partial t}+v_x\frac{\partial v_x}{\partial x}+v_y\frac{\partial v_x}{\partial y}\right)=-\frac{\partial p}{\partial x}+\mu\frac{\partial^2 v_x}{\partial z^2}, \tag{1}$$

where ρ, v_x, v_y, p, μ are density, velocities, pressure, and viscosity, respectively. The dilatation in the film has been neglected as its order of magnitude is of h^2 $(h \ll 1)$.[5]
The typical order of magnitude of the physical parameters that describe the gas squeeze film phenomenon, in units of cm, kg, and s, is

$$L \cong 1,\ h \cong 10^{-3},\ t \cong 10^{-4},\ v_x \cong 10^3,\ v_y \cong 10^3,\ \nu \cong 10^{-1}, \tag{2}$$

where ν is the kinematical viscosity of the gas (air in our case). It follows that the order of magnitude of the terms in Eq. (1) can be indicated by the order of the exponential power, shown under each term

$$\underset{(3+4)}{\frac{\partial v_x}{\partial t}} + \underset{(3+3)}{v_x \frac{\partial v_x}{\partial x}} + \underset{(3+3)}{v_y \frac{\partial v_x}{\partial y}} = -\frac{1}{\rho}\frac{\partial p}{\partial x} + \underset{-1+3+(2\times 3)}{\nu \frac{\partial}{\partial z}\left(\frac{\partial v_x}{\partial z}\right)}. \tag{3}$$

It is clearly seen in Eq. (3) that convective acceleration terms are smaller by 2 orders in comparison with the viscous term. Therefore, it is reasonable to neglect the contribution of the inertia forces associated with the convective acceleration to the pressure gradients.

Commonly in lubrication problems, the considered oscillation frequency of the fluid in the bearing does not exceed a magnitude of 10^3 Hz; therefore, the local acceleration term is ignored as well as the convective acceleration terms. However, when the oscillations are in the range of 10^4 Hz or more (as it is the case for this device), the local acceleration term in Eq. (3) is no longer negligible as it is of a comparable magnitude with the viscous term.

On the other hand, when levitation is considered, the film thickness is determined by equilibrium of forces in the system and cannot be initially prescribed. For relatively large levitated weight, the film thickness could decrease to such an extent that the local acceleration term will be negligible in comparison with the viscous term, even though high oscillation frequency exists.

If only the local acceleration term is considered, Eq. (1) may be reduced to

$$\frac{\partial p}{\partial x} + \rho \frac{\partial v_x}{\partial t} = \mu \frac{\partial^2 v_x}{\partial z^2}. \tag{4}$$

The boundary conditions for a squeeze film between two surfaces with the presence of relative lateral velocity and acceleration are

$$v_x(z=0)=0 \quad v_x(z=h)=\dot{u} \tag{5a}$$

$$\frac{\partial v_x}{\partial t}(z=0)=0 \quad \frac{\partial v_x}{\partial t}(z=h)=\ddot{u}, \tag{5b}$$

where $h=h(x,t)$ is the film thickness and $\dot{u}$, $\ddot{u}$ are the relative lateral velocity and acceleration, respectively.

Gross has suggested that the distribution of acceleration across the film thickness may be assumed as linear.[6] Results obtained using this simplified formulation were in good agreement with those obtained when this restricting assumption was not made. For an assumed linear acceleration profile, together with the boundary conditions in Eq. (5b), Eq. (4) could be written as

$$\frac{\partial p}{\partial x} + \rho \ddot{u}\frac{z}{h} = \mu \frac{\partial^2 v_x}{\partial z^2}. \tag{6}$$

The solution of the differential Eq. (6) under the boundary conditions in Eq. (5a) takes the form

$$v_x(z) = \frac{z}{2\mu}\frac{\partial p}{\partial x}(z-h) + \dot{u}\frac{z}{h} + \ddot{u}\frac{\rho z}{6\mu h}(z^2-h^2). \tag{7}$$

Equation (7) shows that the fluid velocity profile depends on the film thickness and the pressure gradient, and is coupled to the motion of the levitated object.

Integrating the continuity equation across the film thickness and rearranging the terms produces

$$\frac{\partial}{\partial x}\int_0^h \rho v_x dz + \frac{\partial}{\partial t}(\rho h) = 0. \tag{8}$$

Substituting the expression for the velocity profile in the gas film, as was derived in Eq. (7), into Eq. (8) produces the compressible Reynolds equation for a gas squeeze film incorporating relative lateral motion and acceleration of the surfaces

$$\frac{\partial}{\partial x}\left(\frac{\rho h^3}{\mu}\frac{\partial p}{\partial x}\right) = 12\frac{\partial}{\partial t}(\rho h) + 6\dot{u}\frac{\partial}{\partial x}(\rho h) - \ddot{u}\frac{\partial}{\partial x}\left(\frac{\rho^2 h^3}{2\mu}\right). \tag{9}$$

The density and the pressure are related by equation of state; hence, nonlinearity is introduced in Eq. (9).

The following analysis can be extended to describe the case of two-dimensional flow with lateral motion between the surfaces in both directions, meaning a relative motion in the *x*,*y* plane as well as in the *z* direction. For such a case, Eq. (9) becomes

$$\begin{aligned}\frac{\partial}{\partial x}\left(\frac{\rho h^3}{\mu}\frac{\partial p}{\partial x}\right) + \frac{\partial}{\partial y}\left(\frac{\rho h^3}{\mu}\frac{\partial p}{\partial y}\right) &= 12\frac{\partial}{\partial t}(\rho h) + 6\dot{u}\frac{\partial}{\partial x}(\rho h) + 6\dot{v}\frac{\partial}{\partial y}(\rho h) \\ &\quad - \ddot{u}\frac{\partial}{\partial x}\left(\frac{\rho^2 h^3}{2\mu}\right) - \ddot{v}\frac{\partial}{\partial y}\left(\frac{\rho^2 h^3}{2\mu}\right),\end{aligned} \tag{10}$$

where $\dot{v}$, $\ddot{v}$ are equivalent to $\dot{u}$, $\ddot{u}$ for the relative motion in the *y* direction. Equation (10) describes the dynamical behavior of the squeezed fluid, taking into account both time- and space-varying gap and relative acceleration. The complete dynamics requires coupling of the floating object to the supporting fluid.

B. The kinematics of the boundary and the air gap

As was mentioned earlier, the film thickness h is determined by equilibrium of forces in the system and is defined by the clearance between the vibrating surface and the levitated surface. Let the vibrating surface be a traveling wave, which vibrates at frequency (ω) with amplitudes (a_1,a_2) and wavelength (λ)

$$f(x,t) = a_1 \sin(\omega t - kx) + a_2 \sin(\omega t + kx), \quad k = 2\pi/\lambda. \tag{11}$$

In order to assure that pressure radiation will take place, the wavelength of the vibrating surface must be larger than the acoustic wavelength in the air film. This means that only above a critical vibrating frequency will levitation take place.

In practice, the mechanical imperfections make it impossible to attain a perfect traveling wave; therefore, the numerical model uses a realistic combination of two traveling waves in opposite directions. As the degree of purity of the excited wave in the positive-*x* direction increases, the standing wave ratio (SWR), which is defined by $\mathrm{SWR}=|a_1+a_2|/|a_1-a_2|$, approaches 1.

The bottom surface (*s*) of the floating object is defined geometrically by the position of the plate. Therefore, the expression describing the bottom surface's line (see Fig. 1) is

$$s(x,u,v,\theta)=v+\tan(\theta)(x-u), \quad x_1<x<x_2. \tag{12}$$

The clearance is described by

$$\begin{aligned} h(x,u,v,\theta,t)&=s(x,u,v,\theta)-f(x,t)\\ &=v+\tan(\theta)(x-u)-a_1\sin(\omega t-kx)\\ &\quad -a_2\sin(\omega t+kx). \end{aligned} \tag{13}$$

The clearance is derived from the position of the plate's center of gravity (u,v) and the plate's angle of inclination (θ), and is varying in space and time. In the present study, it is assumed that the vibrating surface is uniform along the y axis and the wave propagates only in the x direction.

C. Floating plate dynamics

Three types of external loads are exerted upon the floating plate: levitation forces, lateral forces, and rotational moments. In this section, these forces will be presented in some detail. The matrix form of the plate's equations of motion has the form

$$\begin{bmatrix} m & 0 & 0\\ 0 & m & 0\\ 0 & 0 & J \end{bmatrix} \begin{Bmatrix} \ddot{u}\\ \ddot{v}\\ \ddot{\theta} \end{Bmatrix} = \begin{Bmatrix} N_1\\ N_2\\ M_1 \end{Bmatrix}, \tag{14}$$

where m is the plate's mass, J is the inertial moment of the plate around its center of gravity, and N_1, N_2, M_1 are the lateral force, the levitation force, and the rotational moment, respectively.

The lateral forces acting on the plate are due to shear stresses in the squeeze film that develop as a result of nonuniformity of the pressure gradients in the lateral direction, and due to the relative motion between the surfaces in the lateral direction. In addition, there is drag force acting on the upper face of the plate.

For a Newtonian flow, the shear stresses in the flow acting on a plane normal to the z axis are defined by

$$\tau_{zx}=\mu\left(\frac{\partial v_z}{\partial x}+\frac{\partial v_x}{\partial z}\right)\cong\mu\frac{\partial v_x}{\partial z}. \tag{15}$$

The fluid velocity in the normal direction v_z could be neglected, as was explained in Sec. II A. Substituting Eq. (7) into Eq. (15) gives the expression for the shear stress on the bottom surface of the floating plate

$$\tau_{zx}|_{z=h}=\mu\left.\frac{\partial v_x}{\partial z}\right|_{z=h}=\frac{h}{2}\frac{\partial p}{\partial x}+\mu\frac{\dot{u}}{h}+\frac{\ddot{u}\rho h}{3}. \tag{16}$$

Equation (16) shows that the shear stresses on the plate consist of three terms. The first term is due to pressure gradients in the film. The second term depends on the relative velocity between the plates. As the relative velocity increases, this component of the stress increases until equilibrium with the pressure gradient is reached. At this stage the plate stops accelerating, the third term in the shear stress vanishes, and the plate continues at terminal steady velocity. In addition, as the film thickness h decreases, the pressure gradients increase and the shear stress in the film increases. This suggests that the terminal velocity may have a maximum value with respect to the film thickness and pressure gradients. The investigation of the dependency is beyond the scope of this paper, since the numerical model is not developed for cases involving relatively small surface densities (weight/area), as will be discussed later on.

The motion of the plate in the surrounding air generates a boundary layer on the exposed surface of the plate. The shear stresses in this boundary layer produce a drag force that resists the plate's motion. This drag force acting on the plate in the case of laminar flow is[7]

$$f_D=\tfrac{1}{2}c_D\rho_a\dot{u}^2Lb, \quad c_D=\frac{1.328}{\sqrt{\mathrm{Re}_L}}, \tag{17}$$

where Reynolds number $\mathrm{Re}_L=\dot{u}L/\nu<5\times10^5$ and ρ_a is the gas density at ambient conditions.

Integrating the shear stress along the plate's length, together with the force created by pressure acting on the plate's projected area normal to the lateral direction, and taking into account the drag force, we obtain the total lateral force (in space) as function of time acting on the plate in the x direction

$$\begin{aligned} N_1=&-\int_{x_1}^{x_2}\int_0^b \tau_{zx}|_{z=h}dy\,dx\\ &-\int_{x_1}^{x_2}\int_0^b (p-p_a)\sin(\theta)dy\,dx-f_D. \end{aligned} \tag{18}$$

Here, ρ_a is the gas pressure at ambient conditions, b is the plate's width, and the negative sign on the shear stress integration is added since the normal of the plate's bottom surface is pointing in the negative-z direction.

The total levitation force on the plate is the difference between the gravitational force of the plate and the force exerted by the stresses in the squeeze film on the plate. For small inclination angle, the viscous terms in the principal stress tensor are three orders of magnitude smaller than the pressure term.[5] Therefore, the total levitation force (in space) as function of time is taken as:

$$N_2=-mg+\int_{x_1}^{x_2}\int_0^b (p-p_a)\cos(\theta)dy\,dx. \tag{19}$$

The total rotational moment (in space) as function of time acting on the center of gravity of the plate around the y axis is defined by

$$M_1=\int_{x_1}^{x_2}\int_0^b (x-u)(p-p_a)dy\,dx. \tag{20}$$

As the plate's inclination is in the order of h/L, which is very small, the moments produced by the lateral components of the pressure are smaller by several orders of magnitudes than those in Eq. (20); therefore, they have no significant contribution to the total moment. This will be shown in Sec. III A, when the normalized equations are presented.

III. THE NUMERICAL ALGORITHM—FORMULATION

The numerical algorithm in this work couples the squeeze film phenomenon, which is represented by means of finite difference equations, together with the equations de-

scribing the dynamics of the floating plate. First, we represent the normalized equations governing the system's dynamics, then we discuss the scheme of the coupled numerical solver.

A. Normalized equations of motion of the system

In order to improve the numerical stability, it is essential to normalize the equations, especially as the dimensions governing the problem may differ by several orders of magnitudes. The dimensionless parameters

$$P=\frac{p}{p_a},\quad \Gamma=\frac{\rho}{\rho_a},\quad H=\frac{h}{h_0},\quad X=\frac{x}{L},\quad Y=\frac{y}{L},\quad T=\omega t, \tag{21}$$

are introduced, where p_a is atmospheric pressure, ρ_a is the gas density at atmospheric pressure, h_0 is the mean clearance between the surfaces, and ω is the oscillation frequency. For gas film in which polytropic flow ($p\rho^{-n}=\text{const}$) is postulated with $n=1$ for isothermal behavior, it is possible to replace Γ by P. The assumption of isothermal behavior is reasonable, as the thickness of the gas film is very thin compared to the bearing surfaces, and the heat capacity of the bearings is much larger than the heat capacity of the film. In the next section a mathematical explanation of the differences between an isothermal model and adiabatic model is provided.

Using the dimensionless parameters, the normalized Reynolds equation for two-dimensional flow with no relative motion in the y direction may be written as

$$\frac{\partial}{\partial X}\left(PH^3\frac{\partial P}{\partial X}\right)+\frac{\partial}{\partial Y}\left(PH^3\frac{\partial P}{\partial Y}\right)=\sigma\frac{\partial}{\partial T}(PH)+\Lambda_X\frac{\partial}{\partial X}(PH)-\alpha_X\frac{\partial}{\partial X}(P^2H^3), \tag{22}$$

where

$$\sigma=\frac{12\omega\mu_0L^2}{p_ah_0^2},\quad \Lambda_X=\frac{6\mu_0L\dot{u}}{p_ah_0^2},\quad \alpha_X=\frac{\rho_aL\ddot{u}}{2p_a},$$

and μ_0 is the gas viscosity at initial state. In order to derive the normalized equations describing the plate's motion, we introduce, in addition to Eq. (21), several dimensionless parameters

$$U=\frac{u}{L},\quad V=\frac{v}{h_0},\quad Z=\frac{z}{h_0},\quad \Theta=\frac{\theta}{\theta_0},\quad B=\frac{b}{L},\quad A_i=\frac{a_i}{h_0},$$

where $\theta_0=h_0/L$. As the inclination angle θ is assumed to be very small, approximating $\sin(\theta)$, $\tan(\theta)\to\theta$, and $\cos(\theta)\to1$ is permissible. The normalized Eq. (13) expressing the local film thickness takes the form

$$H=V+\frac{\Theta\,\theta_0L}{h_0}(X-U)-A_1\sin(T-kXL)-A_2\sin(T+kXL). \tag{23}$$

The normalized version of Eq. (14), describing the plate's motion, is

$$\begin{Bmatrix}\frac{\partial^2U}{\partial T^2}\\ \frac{\partial^2V}{\partial T^2}\\ \frac{\partial^2\Theta}{\partial T^2}\end{Bmatrix}=\begin{Bmatrix}-\int_{X_1}^{X_2}\int_0^B\left(\Phi_1H\left(\frac{\partial P}{\partial X}\right)+\Phi_2\frac{1}{H}\left(\frac{\partial U}{\partial T}\right)+\Phi_3PH\left(\frac{\partial^2U}{\partial T^2}\right)+\Phi_4(P-1)\Theta\right)dY\,dX-\Phi_5\left|\frac{\partial U}{\partial T}\right|^{1/2}\left(\frac{\partial U}{\partial T}\right)\\ -G+\Phi_6\int_{X_1}^{X_2}\int_0^B(P-1)dY\,dX\\ \Phi_7\int_{X_1}^{X_2}\int_0^B(X-U)(P-1)dY\,dX,\end{Bmatrix}, \tag{24}$$

where the dimensionless constants are

$$\Phi_1=\frac{h_0p_a}{2m\omega^2},\quad \Phi_2=\frac{\mu_0L^2}{h_0m\omega},\quad \Phi_3=\frac{\rho_ah_0L^2}{3m},$$

$$\Phi_4=\frac{p_a\theta_0L}{m\omega^2},\quad \Phi_5=0.664\frac{Lb}{m}\sqrt{\frac{\rho_a\mu_0}{\omega}},\quad G=\frac{g}{\omega^2h_0},$$

$$\Phi_6=\frac{p_aL^2}{m\omega^2h_0},\quad \Phi_7=\frac{12p_aL^3}{m(L^2+c^2)\omega^2\theta_0}.$$

Note that the second time derivative of U appears also in the expression of the lateral force. This will be treated in Sec. III B, where the formulation of the numerical solver is discussed.

If the moments produced by lateral components of the pressure forces were taken into consideration, it would have resulted in an additional dimensionless constant that would be similar to Φ_7 with the distinction that L^3 in the numerator would be replaced by $L^2h_0\theta_0$. As h_0 and θ_0 are several orders smaller than L, these moments will have no significant contribution to the total moment.

B. Solving the coupled equations of motion numerically

The dynamical behavior of the current system consists of the plate's dynamics coupled with compressible flow effects of the squeeze film. The equations of motion, being nonlinear, need to be integrated numerically in time to obtain the overall solution that incorporated the mutual coupling between the subsystems.

The numerical algorithm consists of two main parts: The first part consists of a finite-difference scheme in space to

descretizing the Reynolds equation. The Reynolds equation requires the instantaneous clearance between the surfaces computed from the instantaneous gap (see Fig. 1) between the floating object and the vibrating part. The initial conditions consist of the position and velocities of the free plate relative to the vibrating surface and the initial pressure distribution in the gas film. The second part of the algorithm incorporates an adaptive time integration of the coupled equations.

In the presented case, there is symmetry in the y axis along the x axis, hence allowing integrating across y from 0 to $B/2$ instead of B. This reduces by half the number of integrated variables and consequently reduces the computational cost.

By application of a finite-difference scheme in space, the Reynolds equation takes the form of a set of ordinary normalized differential equations in time

$$\begin{aligned}\sigma\left(\frac{\partial P}{\partial T}\right) &= -\sigma\frac{P_{i,j}}{H_{i,j}}\left(\frac{\partial H}{\partial T}\right)_{i,j} + H_{i,j}^2\left[\left(\frac{\partial P}{\partial X}\right)_{i,j}^2 + \left(\frac{\partial P}{\partial Y}\right)_{i,j}^2\right] \\ &+ P_{i,j}H_{i,j}^2\left[\left(\frac{\partial^2 P}{\partial X^2}\right)_{i,j} + \left(\frac{\partial^2 P}{\partial Y^2}\right)_{i,j}\right] \\ &+ 3P_{i,j}H_{i,j}\left[\left(\frac{\partial P}{\partial X}\right)_{i,j}\left(\frac{\partial H}{\partial X}\right)_{i,j} + \left(\frac{\partial P}{\partial Y}\right)_{i,j}\left(\frac{\partial H}{\partial Y}\right)_{i,j}\right] \\ &- \Lambda_X\left[\left(\frac{\partial P}{\partial X}\right)_{i,j} + \frac{P_{i,j}}{H_{i,j}}\left(\frac{\partial H}{\partial X}\right)_{i,j}\right] \\ &+ \alpha_X\left[2P_{i,j}H_{i,j}^2\left(\frac{\partial P}{\partial X}\right)_{i,j} + 3P_{i,j}^2H_{i,j}\left(\frac{\partial H}{\partial X}\right)_{i,j}\right]. \quad (25)\end{aligned}$$

The double-subscript notation i,j indicates the grid coordinate on the plane x,y, respectively. The spatial derivatives of the pressure are expressed by central-difference approximation, and the film thickness with its spatial and time derivatives are derived analytically from Eq. (23). The nondimensional parameters depend on the normalized velocity and acceleration of the plate

$$\sigma = \frac{12\omega\mu_0 L^2}{p_a h_0^2}, \quad \Lambda_X = \frac{6\mu_0\omega L^2}{p_a h_0^2}\dot{U}, \quad \alpha_X = \frac{\rho_a\omega^2 L^2}{2p_a}\ddot{U}.$$

We notice that the squeeze film is coupled with the floating plate not only by the film thickness but also by the plate's motion.

The initial state of the pressure between the plate and the vibrating surface is assumed atmospheric. The boundary conditions on the plate's edges are assumed as pressure release, meaning that the pressure near the edges of the plate is atmospheric. In practice, in cases where the excitation surface is larger than the levitating surface, the pressure on the boundaries is higher than the atmospheric pressure due to acoustic pressure radiation created by the vibrating surface. The influence of the acoustic pressure radiation on the boundaries is significant only for relatively light levitated objects when the pressure gradients in the squeeze film are small. This influence is discussed in the next section. The suitable boundary conditions (b.c.) and initial conditions (i.c.) are

$$\text{b.c.:} \quad P(X,Y,T) = 1, \quad \text{for } X,Y, \text{ on the edges}$$

$$\text{i.c.:} \quad P(X,Y,T=0) = 1.$$

Once more, application of a finite-difference scheme in space brings Eq. (25) to the form of a set of ordinary second-order normalized differential equations in time

$$\begin{Bmatrix}\ddot{U}\\ \ddot{V}\\ \ddot{\Theta}\end{Bmatrix} = \begin{Bmatrix} \dfrac{-\sum_{i,j}\left[\Phi_1 H_{i,j}\left(\dfrac{\partial P}{\partial X}\right)_{i,j} + \Phi_2\dfrac{\dot{U}}{H_{i,j}} + \Phi_4(P_{i,j}-1)\Theta\right]\Delta Y\Delta X - \Phi_5|\dot{U}|^{1/2}\dot{U}}{1+\Phi_3\Sigma_{i,j}(P_{i,j}H_{i,j})\Delta Y\Delta X} \\ -G + \Phi_6\sum_{i,j}(P_{i,j}-1)\Delta Y\Delta X \\ \Phi_7\sum_{i,j}[(X_i-U)(P_{i,j}-1)]\Delta Y\Delta X \end{Bmatrix}. \quad (26)$$

The equations of motion of the system, with consideration of the coupling effects, can be described by a state-space formulation. By defining the state-space variables vector $q = \{U,\dot{U},V,\dot{V},\Theta,\dot{\Theta},P\}^T$, the coupled state-space formulation of the entire system can be produced with Eq. (25) and Eq. (26).

IV. VERIFICATION OF THE ALGORITHM

In order to verify the validity of the numerical algorithm, we degenerate the presented case to the case of standing wave with an infinite wavelength by assigning $A_2 = 0$ and setting $k = 0$. Under these conditions, the formulation reduces to the case of a flat vibrating surface where only levitation force is exerted on the floating object. Such a case was recently investigated numerically and experimentally by Nomura *et al.* and by Minikes and Bucher.[5,8]

The study conducted by Nomura *et al.* was for the case of a vibrating flat (rigid) circular piston acting as a sound source levitating a circular disk.[5] The levitated disk is assumed to be stationary, where in reality the disk would vibrate in response to the source motion. This assumption does

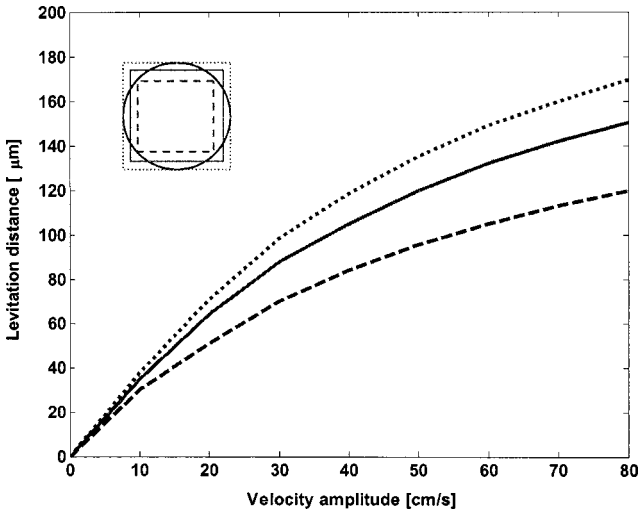

FIG. 2. Levitation distances as function of velocity amplitude the source. Solid curve: equivalent surface area; dashed curve: blocking square, dotted curve: blocked square.

not hold for a heavy levitated object, where the inertial forces of the object must be considered. In the present work there is no such restricting assumption. Additionally, Nomura *et al.* have used an adiabatic relation for a compressible fluid, while in the present work an isothermal behavior was considered. Nomura *et al.* have emphasized the influence of energy leakage on the boundaries by adopting a nonreflection condition of waves.[5] The numerical and experimental results obtained by Nomura *et al.* suggest that the energy leakage does influence the levitation distance for objects with relatively small surface densities (in the range of 1–10 [kg/m^2]). But, the results also suggest that as the surface density is increased, the influence of energy leakage decreases and the use of pressure release boundary conditions becomes suitable.[5]

The presented formulation is carried out for rectangular objects using Cartesian coordinates, while Nomura *et al.* formulated an axisymmetric model for circular objects. Therefore, the comparison is done for the same surface density but with an equivalent square surface. In addition, two bounding squares are simulated and thus the upper and lower limits are obtained by means of a square surface blocking the circular surface and a square surface blocked by the circular surface. Figure 2 shows the numerical results of the levitation distances of a square plate versus the velocity amplitudes of a vibrating source. The vibrating source has the same surface dimensions as the floating square plate, and the values of the physical and numerical parameters, under which the comparison was carried out, are summarized in Table I.

The numerical results presented in Fig. 2 are in a good agreement with the numerical and experimental results provided by Nomura *et al.*[5] We have also simulated the discussed case with an axisymmetric formulation introduced in Minikes and Bucher, where a better agreement has been achieved as the bearings geometries were identical.[8]

It is reasonable to expect differences in the results between a model assuming isothermal behavior and a model under an adiabatic behavior assumption. As was discussed in Sec. III A, for a gas film in which an isothermal polytropic flow ($p\rho^{-1}=\text{const}$) is postulated, it is possible to replace Γ by P to obtain Eq. (22). But, when adiabatic behavior is postulated, the relation between the normalized pressure and the normalized density is $\Gamma=P^{1/n}$, with $n=C_P/C_V=1.4$ for air. In such case, Eq. (22) will take the form

$$\frac{\partial}{\partial X}\left(\frac{P^{1/n}H^3}{\tilde{\mu}}\frac{\partial P}{\partial X}\right)+\frac{\partial}{\partial Y}\left(P^{1/n}H^3\frac{\partial P}{\partial Y}\right)$$
$$=\sigma\frac{\partial}{\partial T}(P^{1/n}H)+\Lambda_X\frac{\partial}{\partial X}(P^{1/n}H)-\alpha_X\frac{\partial}{\partial X}(P^{2/n}H^3). \tag{27}$$

The dimensionless parameter $\tilde{\mu}=\mu/\mu_0$ is the normalized viscosity, as it is not constant. Inspecting the analysis results of an isothermal model with the physical dimensions used in the comparison to Nomura *et al.*, it appears that the fluctuations of the normalized pressure are no more than 10%–20%. In such case, the normalized density $\Gamma=P^{1/1.4}\approx P$, as the values of P are close to 1. In addition, it is reasonable to assume that the transient period for reaching steady state is too short for allowing any thermal changes to occur, meaning that the viscosity remains constant at $\tilde{\mu}=1$. Under the above conditions, Eq. (27) may be reduced to Eq. (22). This may provide an explanation why differences in the analysis results are minor. Nevertheless, a detailed thermodynamical study is required for fully understanding the squeeze film behavior.

TABLE I. Values of the physical and numerical parameters used in the comparison with Nomura *et al.* (Ref. 5).

Parameter	Value
R_0—Disk radius	20 [mm]
L—Square's face	
Equivalent surface	$L=\sqrt{\pi}R_0$
Blocked square	$L=\sqrt{2}R_0$
Blocking square	$L=2R_0$
c—Disk thickness	2 [mm]
m—levitated mass	7.4 [gm]
ω—Frequency	19.5 [kHz]
A_1—Vibration amplitude	6.54 [μm]
ΔX—Grid interval	0.05
ΔY—Grid interval	0.05
μ_0—Air viscosity	17.9 [N·s/mm^2]
ρ_0—Air density	1 [Kg/m^3]
p_a—Ambient pressure	101 [kPa]

V. STUDYING THE SENSITIVITY OF THE SYSTEM

In this section we study the influence of several physical parameters on the behavior of the system, especially the influence on the lateral terminal velocity of the levitated object. The parameters are the standing wave ratio (SWR), the ratio between the plate's length and the wavelength (L/λ), the average vibration amplitude of the excitation surface, and the influence of the acoustic pressure radiation on the boundaries. The physical parameters and the numerical parameters under which the simulations were carried out are summarized in Table II.

TABLE II. Values of the physical and numerical parameters used in the numerical investigation.

Parameter	Value
L—Plate length	90 [mm]
b—Plate width	65 [mm]
c—Disk thickness	2.25 [mm]
ω—Frequency	19.5 [kHz]
A_1—Vibration amplitude	7.5 [μm]
p_a—Ambient pressure	101 [kPa]
μ_0—Air viscosity	17.9 [N·s/mm^2]
ρ_0—Air density	1 [Kg/m^3]
ΔX—Grid interval	0.025
ΔY—Grid interval	0.111

A. Terminal speed versus standing wave ratio (SWR)

As mentioned earlier, mechanical imperfections in a system make it almost impossible to attain a pure traveling wave. Therefore, there is a significant importance to investigate the response of the system to various standing wave ratios (SWR). Figure 3 presents the terminal velocity of the levitated plate in the presence of different SWR. The numerical results were obtained for three levitated plates with different surface densities (σ_D[kg/m^2]), and the ratio of the plate's length to wavelength (L/λ) was set to 2.37.

The numerical simulation suggests that the terminal speed of the levitated plate decreases as the ratio between the maximum amplitude and the minimum amplitude (SWR) increases. The relation between the terminal velocity and the SWR is linear when plotted on logarithmic scale. In addition, Fig. 3 indicates that the higher the surface density the lower the terminal speed of the levitated plate.

B. Terminal speed versus wavelength

When designing a system for generating traveling waves, the imposed boundary conditions make it difficult to obtain a perfect sinusoidal wave with a prescribed wavelength. Moreover, it is desired to transport plates of different lengths. Therefore, we have chosen to introduce the response

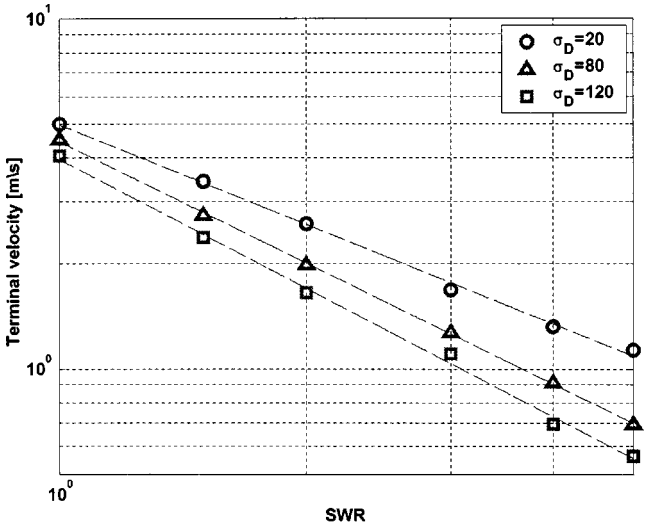

FIG. 3. Terminal velocity versus the standing wave ratio for different surface densities: σ_D=20,80,120 [Kg/m^2].

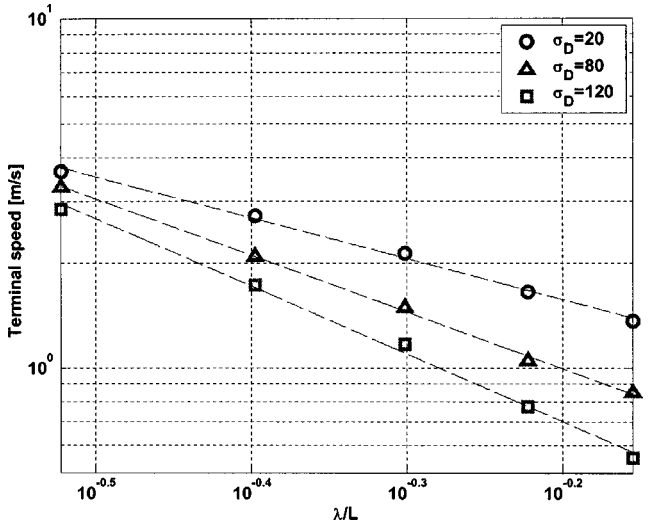

FIG. 4. Terminal velocity versus wavelength of the traveling wave for different surface densities: σ_D=20,80,120 [Kg/m^2].

of the system to the ratio between the length of the levitated plate and the wavelength of the excited traveling wave. Figure 4 presents the terminal velocity of the levitated plate for different ratios (L/λ). The numerical results were obtained for three levitated plates with different surface densities and the SWR was set to 2.

The numerical simulation suggests that the terminal speed of the levitated plate decreases as the ratio (λ/L) between the wavelength of the excited traveling wave and the plate's length increases. This relation appears to be linear when plotted on a log–log scale. In addition, as in Fig. 3, Fig. 4 indicates that the higher the surface density the lower the terminal speed of the levitated plate.

C. The pressure field and the influence of boundary conditions

Figure 5 shows how the pressure distribution in a cross section of the squeeze film varies with time for the case of excitation by a traveling wave. Two cases are presented: (a) surface density of 1.5 [Kg/m^2]; (b) surface density of 80 [Kg/m^2]. The average inclination of the plate in case (a) is Θ=12, while the average inclination of the plate in case (b) is nearly zero. As can be seen in Fig. 5(a), the pressure values on the leading edge of the plate is smaller than on the lagging edge, while in Fig. 5(b) the pressure are almost equally distributed. It appears from the numerical simulations that the average angle of attack of the plate increases as the surface density decreases.

The vibration amplitude was chosen to be 10 [μm] and the SWR was set to 2 (all the other physical and numerical parameters appear in Table II). Figure 5 shows that as the pressure distribution progresses in time, its amplitudes oscillate between maximum and minimum. This is a direct result of having a standing wave ratio greater than 1, which is obviously not a pure traveling wave.

The squeeze film equilibrium is established through a balance between viscous flow forces and compressibility forces. The pressure in the boundaries of the levitated plate influences the pressure gradients introduced in the film. The

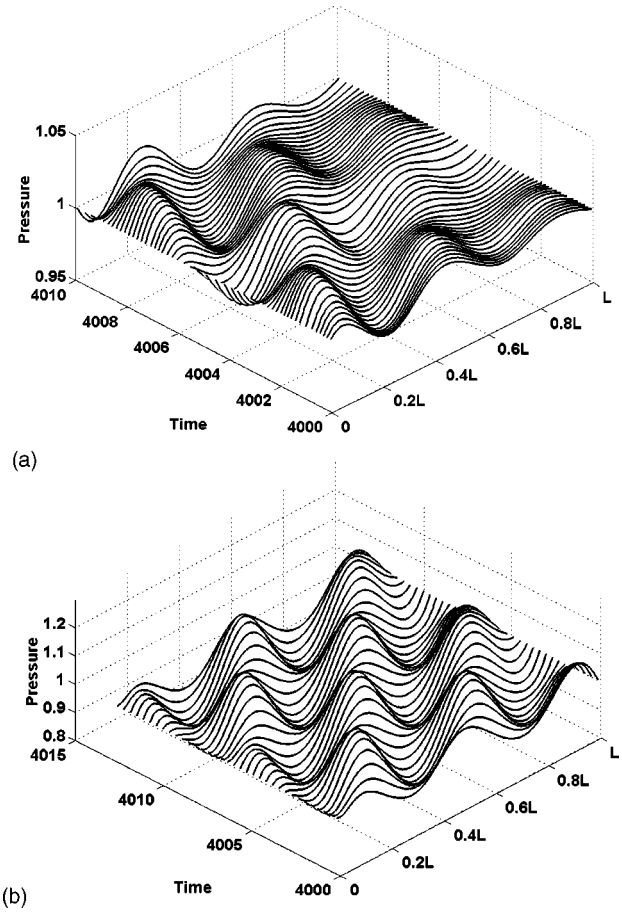

FIG. 5. Normalized pressure distribution in a cross section of the squeeze film varies with time (normalized). (a) surface density 1.5 [Kg/m^2]; (b) surface density 80 [Kg/m^2].

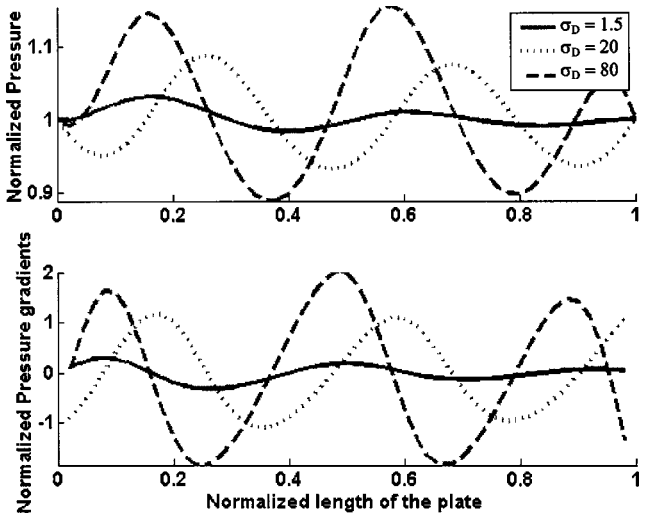

FIG. 6. Normalized pressure and gradients in a cross section of the squeeze film at an arbitrary point in time. Solid curve: surface density 1.5 [Kg/m^2], dotted curve: surface density 20 [Kg/m^2]; dashed curve: surface density 80 [Kg/m^2].

thickness of squeeze film is on the order of magnitude of a few hundreds of microns, which is much smaller than the radiated acoustic wavelength (several millimeters at 19 [kHz]). Therefore, the edges of the levitated plate are close to the vibrating surface and are exposed to mean radiation pressure higher than the ambient pressure.[8,9] The pressure values near the peripheries of the levitated object (which determine the boundary conditions) may indeed influence the film thickness and consequently the dynamical behavior.

For the load-carrying phenomenon to take place, the pressure gradients in the squeeze film must increase as the surface density of the levitated object increases. This is simply because the force excreted by the film pressure must sustain the weight of the levitated object. The influence of small changes in the radiation pressure near the boundaries decreases with the growth of the pressure gradients in the film. This implies that as the surface density of the levitated plate increases, the system dynamical behavior is less sensitive to changes in the radiation pressure near the boundaries. Figure 6 shows the normalized pressure and the normalized pressure gradients, respectively, in a cross section of the squeeze film at an arbitrary point in time (at steady state). The curves represent different levitated surface densities.

Comparing the different curves in Fig. 6, we notice that the pressure gradients in the case where the surface density is 1.5 [Kg/m^2] are significantly smaller than the pressure gradients in the case where the surface density is 80 [Kg/m^2]. Therefore, in the case of large surface densities, the pressure gradients in the film are hardly affected by a small change in the acoustic radiation pressure near edges of the levitated plate. Since the shear stresses on the levitated plate are associated with the pressure gradients in the film, the levitated distance and the terminal velocity of plates with large surface densities will hardly be affected.

VI. DISCUSSION AND CONCLUSIONS

The presented system has a complex behavior, which is governed by numerous physical parameters. We have shown that the theoretical formulation of system's dynamical behavior introduces some useful relations between the governing parameters. The simulation results suggest that the terminal velocity of the levitated plate is strongly influenced by the standing wave ratio (SWR) and the wavelength of the excitation traveling wave. The terminal velocity decreases with the increase of SWR or with the increase of the ratio (λ/L). In addition, we presented the pressure distribution in a cross section of the squeeze film and the effect of surface density on the plate's angle of attack. We concluded that the acoustic radiation pressure on the boundaries of the levitated plate is significant only for levitated plates with relatively small surface density. For such objects the pressure gradients in the squeeze film are small and therefore sensitive to pressure changes near its peripheries. The acoustic radiation pressure near the vibrating surface must be obtained in order to determine more accurately the extent of its influence on the system behavior.

The assumption made in the numerical model that the levitated plate behaves as a rigid body could deteriorate the validity of the numerical simulations. The flexibility of the levitated plate could have effects on the system dynamical behavior; therefore, a future investigation may focus on the combined dynamical behavior, which incorporates a flexible floating plate.

[1] E. O. J. Salbu, ''Compressible squeeze films and squeeze bearings,'' J. Basic Eng. **86**, 355–366 (1964).
[2] W. Wiesendanger, U. Probst, and R. Siegwart, ''Squeeze film air bearings using piezoelectric bending elements,'' in Proceedings of Fifth International Conference on Motion and Vibration Control (MOVIC2000), Sydney, Australia, pp. 181–186 (2000).
[3] Y. Hashimoto, Y. Koike, and S. Ueha, ''Transporting objects without contact using flexural traveling waves,'' J. Acoust. Soc. Am. **103**(6), 3230–3233 (1998).
[4] B. T. Chu and R. E. Apfel, ''Acoustic radiation pressure produced beam of sound,'' J. Acoust. Soc. Am. **72**(6), 1673–1687 (1982).
[5] H. Nomura, T. Kamakura, and K. Matsuda, ''Theoretical and experimental examination of near-field acoustic levitation,'' J. Acoust. Soc. Am. **111**(4), 1578–1583 (2002).
[6] W. A. Gross, *Gas Film Lubrication* (Wiley, New York, 1962).
[7] R. W. Fox and A. T. McDonald, *Introduction to Fluid Mechanics* (Wiley, New York, 1985).
[8] A. Minikes and I. Bucher, ''Coupled dynamics of a squeeze-film levitated mass and a vibrating piezoelectric disk—numerical analysis and experimental study,'' J. Sound Vib. (in press).
[9] M. P. Norton, *Fundamentals of Noise and Vibration Analysis for Engineers* (Cambridge University Press, Cambridge, 1989).